



The influence of inorganic materials on the pyrolysis of polytetrafluoroethylene. Part 2: The common oxides of Al, Ga, In, Zn, Cu, Ni, Co, Fe, Mn, Cr, V, Zr and La

G.J. Puts*, P.L. Crouse

Department of Chemical Engineering, University of Pretoria, Pretoria 0002, South Africa

ARTICLE INFO

Article history:

Received 21 May 2014

Received in revised form 13 August 2014

Accepted 15 August 2014

Available online 27 August 2014

Keywords:

PTFE pyrolysis

PTFE thermal degradation

Filled PTFE

Catalytic pyrolysis

TGA-FTIR

ABSTRACT

The thermal decomposition of PTFE intimately mixed with the common oxides of selected metals (Al_2O_3 , Ga_2O_3 , In_2O_3 , ZnO , CuO , NiO , Co_3O_4 , Fe_2O_3 , Mn_2O_3 , Cr_2O_3 , V_2O_5 , ZrO_2 and La_2O_3) was investigated by TGA-FTIR. Except for ZrO_2 , all the oxides undergo reaction with PTFE to produce some CO_2 . CuO and V_2O_5 react in bulk and speed up the degradation rate with V_2O_5 also lowering the mass-loss onset temperature by 60 °C. Al_2O_3 moderately increases the yield of hexafluoropropylene and hexafluoroethane.

© 2014 Elsevier B.V. All rights reserved.

1. Introduction

In a previous paper [1] we reported initial results regarding the effects that the sulfates and fluorides of selected fourth period metals have on the degradation rate and gaseous product distribution of PTFE under pyrolysis conditions, as studied by TGA-FTIR. Findings of interest were the observations that AlF_3 , $\text{Al}_2(\text{SO}_4)_3$ and NiSO_4 significantly increase the yield of hexafluoropropylene (HFP), with AlF_3 producing almost exclusively HFP and hexafluoroethane (HFE). Other observations include the formation of waxy substances in the presence of CuSO_4 and CoSO_4 .

In this article we relate the initial results regarding the effects that oxides of Al, Ga, In, Zn, Cu, Ni, Co, Fe, Mn, Cr, V, Zr, and La have on the degradation rate and gaseous product distribution of PTFE under pyrolysis conditions, again as observed by TGA-FTIR.

The oxides investigated here do not display identical coordination numbers as the metals are present in their most common oxidation states. The group 13 elements are in the 3+ oxidation state, Zn, Ni and Cu are in the 2+ oxidation state, Fe, Mn, Cr, and La are in the 3+ oxidation state, Zr is in the 4+ oxidation

state, and V is in 5+. Co is present here as a mixed oxide, containing both Co^{2+} and Co^{3+} .

2. Results and discussion

2.1. Thermal behaviour of pure PTFE

The thermal behaviour of pure PTFE was used as a baseline for the filled PTFE experiments. The thermograms presented in Fig. 1 have been previously discussed [1], but are reproduced here for ease of reference.

The bulk degradation onset temperature was found to be in the region 560 °C with no residue remaining in the crucible after the experiment. The temperature derivatives of the thermograms of Fig. 1 are presented in Fig. 2. From these derivatives the temperature at which mass loss is first noted was found to be 450 °C.

The infrared spectrum of the gas phase, taken at the point of maximum total absorbance, is reproduced in Fig. 3. The spectrum shows the absorption bands for tetrafluoroethylene (TFE) at 1325 and 1183 cm^{-1} along with some minor absorption peaks for HFP at 1787, 1387 and 1033 cm^{-1} .

It should be noted that there are some deviations between the mass loss curves presented in Fig. 1. These deviations are attributed to the effects of polymer particle morphology on the

* Corresponding author. Tel.: +27 12 420 2670.

E-mail address: Gerard.Puts.UP@gmail.com (G.J. Puts).

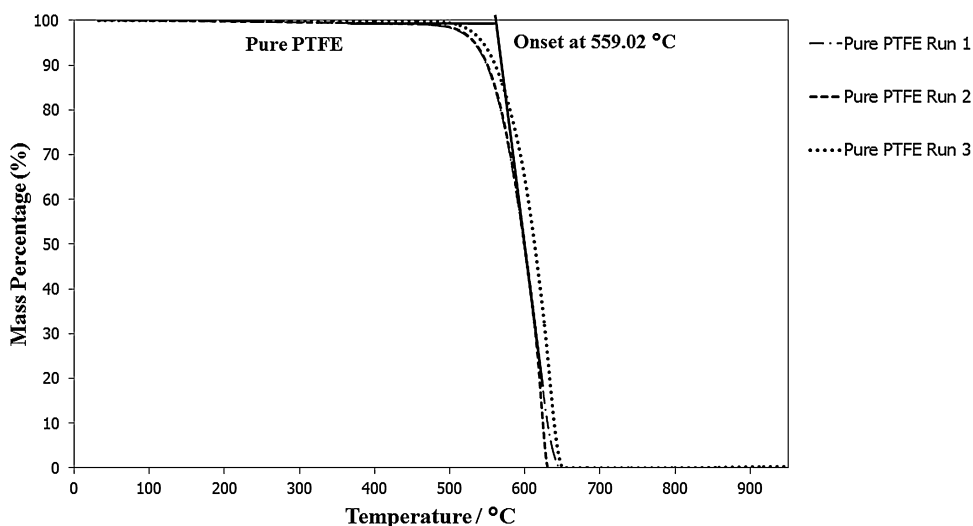


Fig. 1. Thermograms for the PTFE control experiments.

rates of evaporation and diffusion of the gaseous products from the bulk material (and thus on the total degradation rate). The raw material manufacturer does not guarantee completely even distribution of powder particle size or particle shape in the shipped product. The three baseline samples were taken from different section of the raw material container and the differences in material morphology between sample sites is evident from both the thermograms and the derivative curves presented in Fig. 2.

However, the distribution of gaseous products are unaffected by the physical morphology of the raw material. The pyrolysis of pure PTFE produces a gaseous mixture consisting mostly of TFE along with some very minor amounts of HFP. From this we may say that any products other than TFE noticed in the gas phase are due to interaction of the pyrolysates with the filler materials.

2.2. Thermal behaviour of PTFE filled with fourth period transition metal oxides

The thermograms for the decomposition of PTFE filled with ZnO, CuO, NiO, Co_3O_4 , Fe_2O_3 , Mn_2O_3 , Cr_2O_3 and V_2O_5 are presented in Fig. 4. The corresponding IR spectra of the gas phase, taken at the point of maximum absorbance, are presented in Fig. 5.

The behaviour of the fourth period metal oxides is interesting in that, except for V_2O_5 , the degradation onset temperature does not

differ significantly from the pure PTFE control case, being 500 °C for V_2O_5 and 560 °C for the others. More interesting is that CuO and V_2O_5 significantly speed up the rate of degradation, as evidenced by the steep slope of the respective degradation curves. The oxides of Fe and Cr show a slight inhibiting effect on the degradation rate.

It should be noted here that while the sample preparation was done quite carefully, the preparation method does not deliver completely homogeneous polymer/filler composites and some scattering about the 50% mark is noticed in the residue values. The errors are within 5% of the expected final composition and the differences between repeat runs of the same PTFE/filler composite was found to be in the order of 2%. The authors consider these differences immaterial to the interpretation of the results.

For Fe_2O_3 the error is more pronounced. This error is attributed to the tendency of the iron oxide particles to agglomerate. These agglomerations are not easily broke up when the filler is mixed with the PTFE and a large difference in residue values is noticed between repeat runs. Nevertheless, the differences in the amount of iron oxide within the PTFE did not affect the gas phase product distribution.

The infrared spectra indicate that only CuO, NiO, Cr_2O_3 and V_2O_5 have an effect on the gaseous product distribution. In addition to the characteristic tetrafluoroethylene (TFE) peaks at 1326 and 1185 cm^{-1} , the CuO filled material exhibits the same side band at

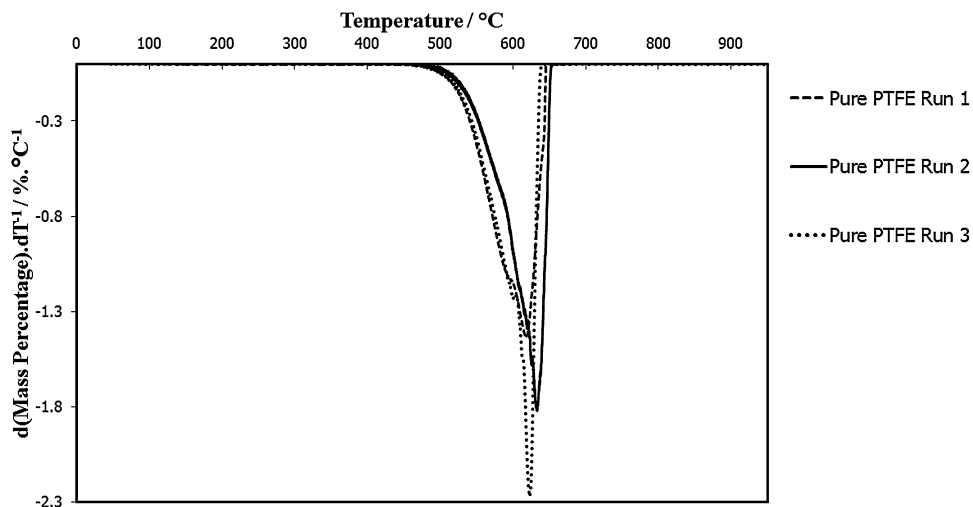


Fig. 2. The temperature first derivatives for pure PTFE.

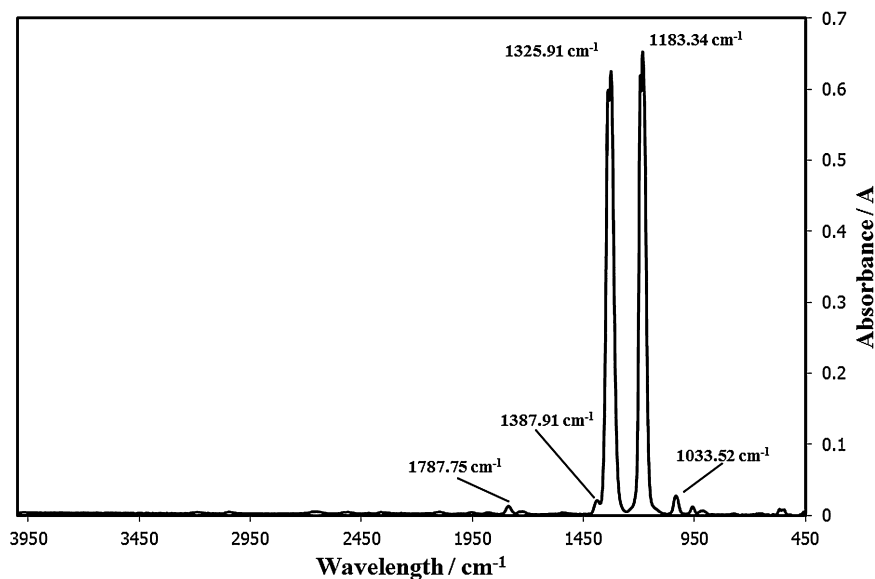


Fig. 3. IR spectrum of the gas phase at maximum absorbance during pyrolysis of pure PTFE.

1245 cm^{-1} that was seen for CuSO_4 [1]. It is also noticed that CuO produces a significant amount of CO_2 , as evidenced by the characteristic absorption band at 2358 cm^{-1} [2].

NiO induces some shouldering in the region of 1245 cm^{-1} , similar to what was observed for the fluorides of the fourth period metals [1], but very little CO_2 . The Cr_2O_3 filled material produces a small peak at 1245 cm^{-1} and no CO_2 . The V_2O_5 filled material produces a large peak at 1028 cm^{-1} and a strong CO_2 absorption band. ZnO, Fe_2O_3 , Co_3O_4 and Mn_2O_3 have no effect on the gas phase other than producing small amounts of CO_2 .

CuO does not undergo oxygen loss under $1000\text{ }^\circ\text{C}$ [3], indicating that the CO_2 observed here is produced by the reduction of CuO by PTFE pyrolysates rather than the combustion of PTFE by free oxygen due to CuO thermal decomposition. This is supported by an *ab initio* study of the reduction of CuO by hydrogen. Maimaiti et al. [4] showed that the (1 1 1) surface, which is the thermodynamically most stable surface of CuO, will readily undergo oxygen abstraction to form first Cu_2O and then Cu metal on the surface.

The fate of the fluorine atoms exchanged in this reduction is unknown at present, but given the presence of the side peak at

1245 cm^{-1} , it is reasonably assumed that they attach themselves to nearby fluorocarbon species, rather than attach to the surface of the CuO crystals.

The observation of waxy residues on the IR transfer line inlet after PTFE pyrolysis in the presence of CoSO_4 or CuSO_4 [1] leads to the conclusion that the species causing the unknown absorption band at 1245 cm^{-1} may be short chain linear fluoroalkanes. The infrared absorption spectra for C_6F_{14} shows a strong absorption band centred 1247 cm^{-1} [2] while C_7F_{16} and C_8F_{18} show a strong absorption band centred at 1254 cm^{-1} [5]. The peak at 1245 cm^{-1} is therefore attributed to one or more short chain perfluoroalkanes.

The absorption band at 1028 cm^{-1} in the V_2O_5 sample is unaccompanied by other absorption bands that correspond to any of the expected pyrolysis or combustion products of PTFE, but does correspond to the characteristic absorption peak for SiF_4 [2]. The X-ray diffraction pattern of V_2O_5 , reproduced in Fig. 6, indicate that the V_2O_5 is crystallographically pure, and X-ray fluorescence shows that there is no silicon present in the inorganic material. This makes the assignment of the 1028 cm^{-1} band to SiF_4 highly implausible.

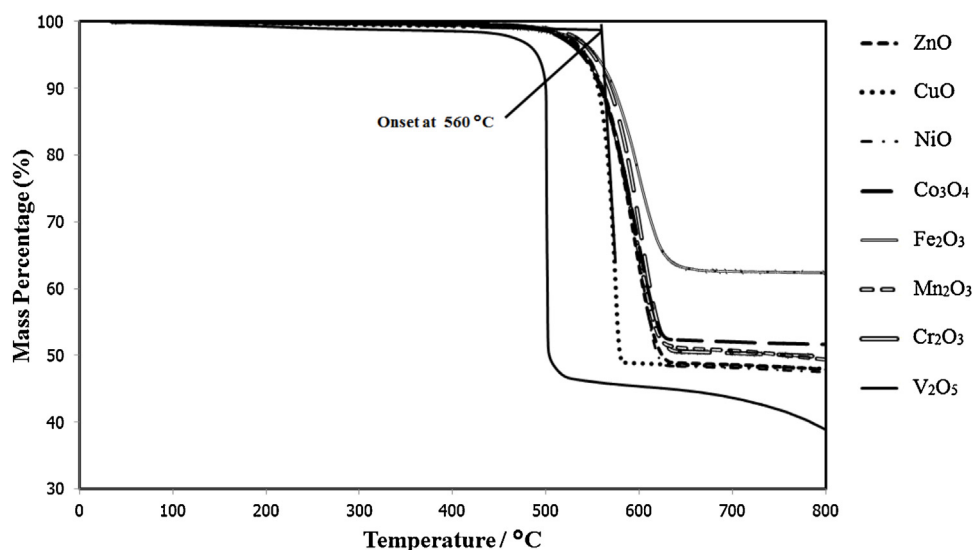


Fig. 4. Thermograms for the decomposition of PTFE filled with ZnO, CuO, NiO, Co_3O_4 , Fe_2O_3 , Mn_2O_3 , Cr_2O_3 and V_2O_5 .

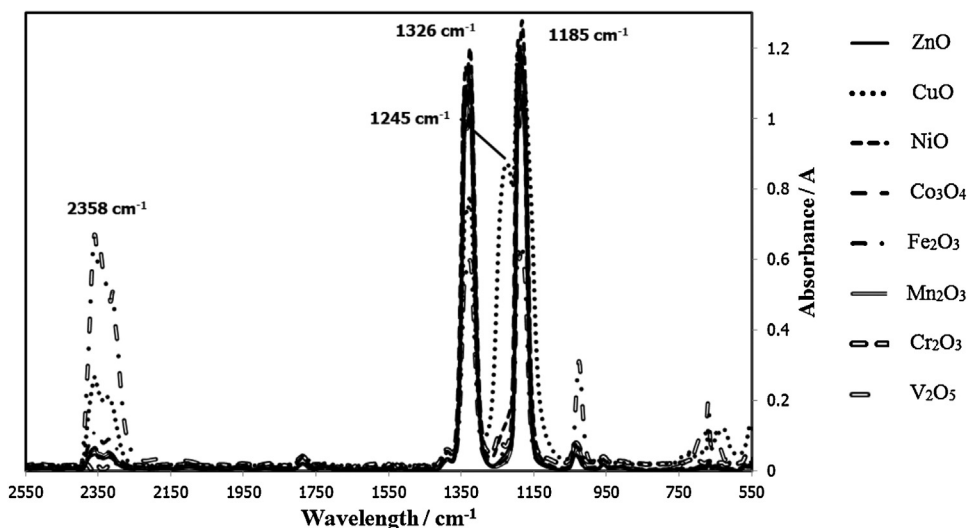


Fig. 5. Infrared spectra of the gas phase, taken at the point of maximum absorbance, for the decomposition of PTFE filled with ZnO, CuO, NiO, Co₃O₄, Fe₂O₃, Mn₂O₃, Cr₂O₃ and V₂O₅.

VF₃ and VF₅ are both volatile at temperatures below 1000 °C, with VF₅ boiling at 111 °C and VF₃ sublimating at 800 °C [3], implying that they could potentially be in the gas phase at PTFE pyrolysis conditions. No literature could be found on the infrared absorption of VF₃. However, the literature indicates that VF₅ does not have any infrared absorbance bands in the region near 1000 cm⁻¹ [6]. Quantum-chemical calculations of VF₃, VF₄ and VF₅ using DFT (B3LYP) with the 6-31+G* basis set indicated that VF₃ has a single absorption band at around 1950 cm⁻¹, VF₄ at around 760 cm⁻¹ and VF₅ exhibiting two absorption bands at around 770 and 830 cm⁻¹ (compare the experimental of 769 and 801 cm⁻¹ [6]). The literature indicates that VF₃O boils at 480 °C [3] and absorbs infrared at 1054, 806, 721.5, 308, 257.8 and 204.3 cm⁻¹ [7]. The absorption behaviour of these compounds indicates that the absorption peak at 1028 cm⁻¹ cannot be due to any vanadium fluoride or vanadium oxyfluoride. The cause of the band at 1028 cm⁻¹ remains unknown at present, but is reasonably assumed to not be caused by SiF₄.

It is known from studies on the thermal decomposition of V₂O₅ that oxygen atoms at the surface of the V₂O₅ crystal become highly labile when the crystal is heated to around 500 °C and that the thermodynamics favour a release of atomic oxygen from the V₂O₅ crystal [8]. Keeping this in mind, the significant increase in degradation rate seen for the pyrolysis of PTFE/V₂O₅ mixtures as well as the significant production of CO₂ is explained *via* the oxidation of the PTFE by atomic oxygen at the polymer/V₂O₅ interface.

2.3. Thermal behaviour of PTFE filled with group 13 oxides

The thermograms for the decomposition of PTFE filled with Al₂O₃, Ga₂O₃ and In₂O₃ are presented in Fig. 7. The corresponding IR spectra of the gas phase, taken at the point of maximum absorbance, are presented in Fig. 8.

The degradation onset temperature is in the region of 550 °C for all three oxides. The rate of degradation for Ga₂O₃ and In₂O₃ does

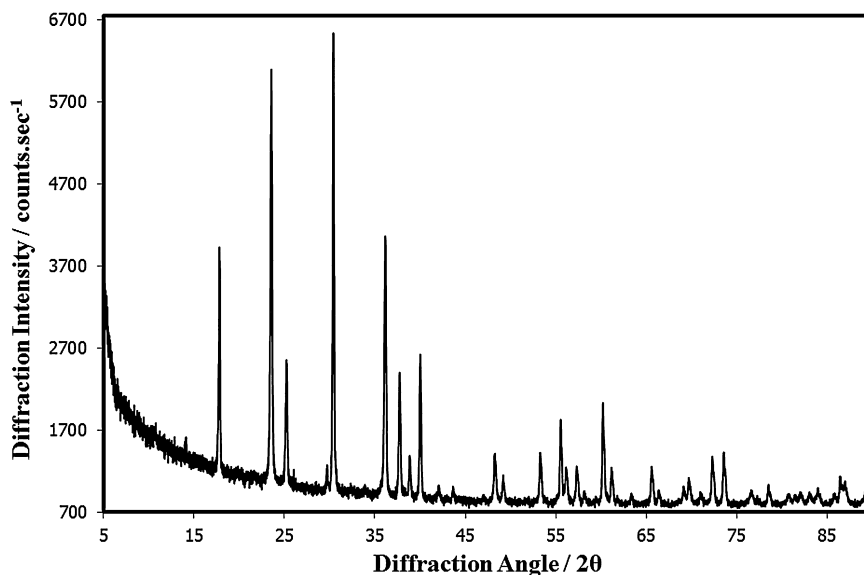


Fig. 6. X-ray diffraction pattern showing the characteristic diffraction peaks for V₂O₅, indicating the V₂O₅ is crystallographically pure.

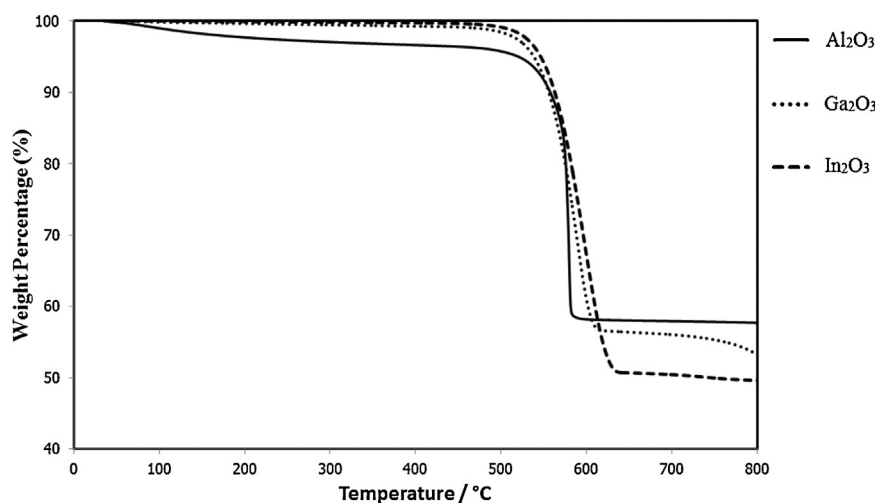


Fig. 7. Thermograms for the decomposition of PTFE filled with Al_2O_3 , Ga_2O_3 and In_2O_3 .

not differ significantly from the control case. However, Al_2O_3 significantly accelerates the degradation rate. Dehydration of the Al_2O_3 is also observed.

The infrared spectra show that Al_2O_3 produces TFE as well as PFE and HFP, similar to what was noticed for AlF_3 and $\text{Al}_2(\text{SO}_4)_3$ [11]. Ga_2O_3 produces some shouldering around 1235 cm^{-1} while In_2O_3 seems to be inert towards the gas phase. Given that all these compounds are Lewis acids, we find that the interaction strength of these compounds with fluorocarbon radicals are of the order of $\text{Al}_2\text{O}_3 \gg \text{Ga}_2\text{O}_3 > \text{In}_2\text{O}_3$.

Studies of the surface of γ -alumina (the phase used in this work) show that the majority of the surface is composed of the (110) facet [9]. There are several metal sites present on the relaxed surface, with the most acidic being the 3-fold coordinated aluminium.

Considering that PTFE degrades *via* the elimination of: CF_2 units [10], a plausible mechanism for the Al_2O_3 catalysed reactions involves the chemisorption of: CF_2 onto the metal sites *via* the insertion of the unpaired electrons into the empty p-orbital of 3 fold co-ordinated metal atoms at the surface of the catalyst crystal. If a situation arises where two CF_2 units can co-ordinate to a central CF_2 , fluorine re-arrangement may occur to produce HFP which then desorbs from the catalyst surface.

Although reactions between aluminium, Al_2O_3 and PTFE are well known in the context of military thermites [11,12], little is known about the intermediates that facilitate these reactions. Pantoya and Dean [11] have observed a “pre-ignition reaction” (PIR) in PTFE/ Al_2O_3 and Onodera et al. [13] have observed reactions between PTFE and Al_2O_3 under friction conditions in QCMD simulations. The results from Onodera et al. indicate transfer of fluorine from the PTFE to the alumina surface to produce fluorine-terminated, fourfold co-ordinated aluminium sites on the Al_2O_3 surface layers. This reaction should be relatively exothermic and the PIR reactions observed by Pantoya et al. strongly supports this exchange of fluorines.

It must be qualified here that there is significant overlap between the work of these two groups as the intimate contact of the nano- Al_2O_3 /PTFE thermite composites approach the intimate contact required by the tribological simulations and the local energy states at the PTFE/ Al_2O_3 interface due to friction approaches the energies require for ignition of the Al_2O_3 /PTFE composite.

In light of the reactions between AlF_3 and PTFE [1], the production of HFP and HFE observed here is found to be due not to a catalytic interaction of the pyrolysates with Al_2O_3 , as described in the preceding paragraphs, but due to an interaction between the AlF sites on the surface of the Al_2O_3 .

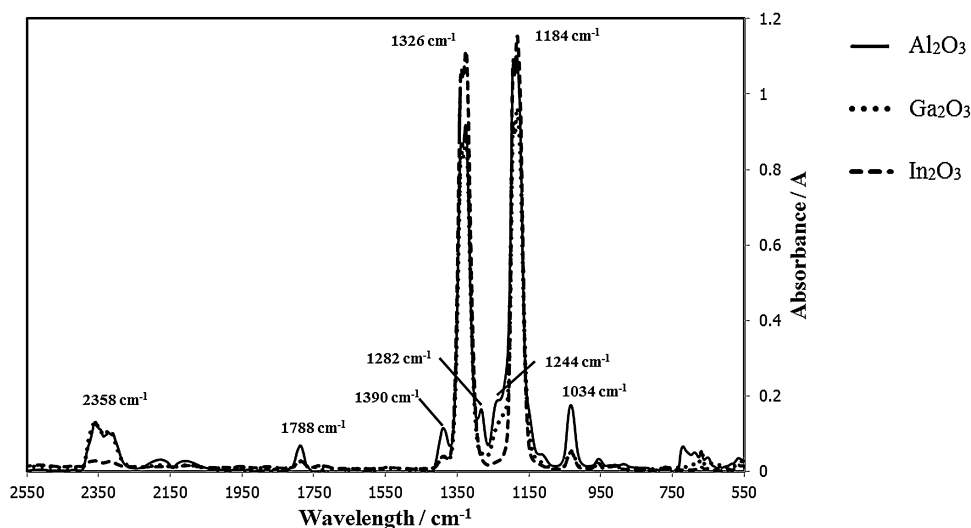


Fig. 8. Infrared spectra of the gas phase, taken at the point of maximum absorbance, for the decomposition of PTFE filled with Al_2O_3 , Ga_2O_3 and In_2O_3 .

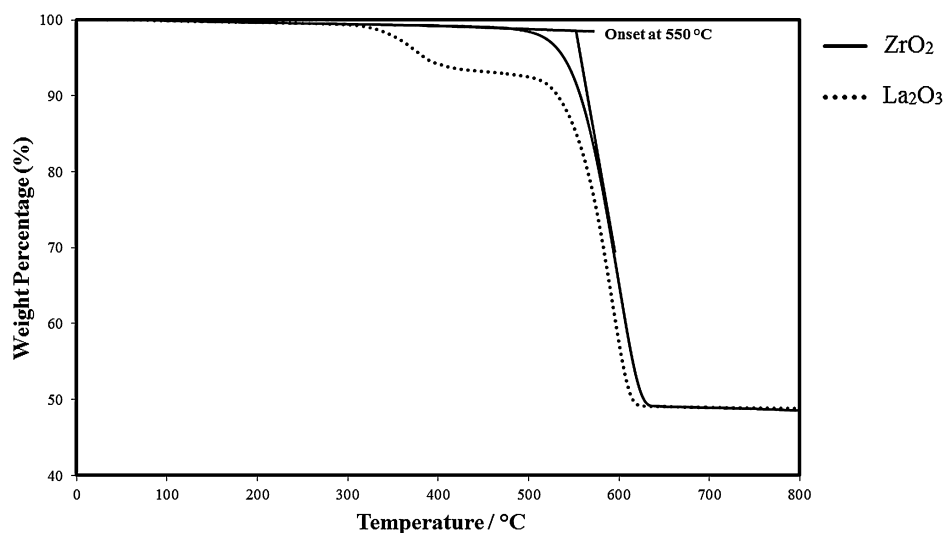


Fig. 9. Thermograms for the decomposition of PTFE filled with ZrO_2 and La_2O_3 .

It stands to reason that the exchange of fluorines between a PTFE and an oxide or metal surface should generate some sort of weakness in the polymer chain. As indicated by Onodera et al. [13], chain scission, rather than the formation of stable carbon radicals on the polymer backbone, should occur and, in the case of the pyrolysis of PTFE with Al_2O_3 , the increase in degradation rate may be explained by the shortening of the polymer chain *via* these scissions.

The behaviour of B_2O_3 could not be studied as the B_2O_3 melt evaporated completely from the crucible before PTFE pyrolysis occurred.

Scattering of the residue value data is noted in Fig. 7. The deviation from the expected 50% mark is again attributed to the formation of difficult-to-break-up agglomerations by the Al_2O_3 and Ga_2O_3 . Also noted in Fig. 7 is the dehydration of Al_2O_3 . While the alumina was initially anhydrous, water absorption occurred during sample preparation due to contact with atmospheric moisture. The amount of water released here indicates the water was adsorbed onto the surface of the alumina. While water is known to retard the pyrolysis of PTFE [14], the amount of water present in the composite at the breakdown temperature of PTFE is such that its effect can be taken as being vanishingly small.

2.4. Thermal behaviour of PTFE filled with ZrO_2 and La_2O_3

The thermograms for the decomposition of PTFE filled with ZrO_2 and La_2O_3 are presented in Fig. 9. The corresponding IR spectra of the gas phase, taken at the point of maximum absorbance, are presented in Fig. 10.

Zirconia and lanthana are known to be generally unreactive, requiring high temperatures and severe conditions to react. The thermograms indicate that this inertness is exhibited in the presence of fluorocarbon radicals as well, with neither ZrO_2 nor La_2O_3 significantly affecting the degradation onset temperature (found to be 550 °C for ZrO_2 and 530 °C for La_2O_3). The slopes of the degradation curves are somewhat flatter than what is observed for pure PTFE, indicating that ZrO_2 and La_2O_3 have an inhibiting effect on the degradation rate.

The infrared spectra indicate that ZrO_2 and La_2O_3 have no effect on the gaseous product distribution other than La_2O_3 producing some CO_2 .

The first decomposition step seen in the La_2O_3 filled PTFE is due to the dehydration of the La_2O_3 as water vapour is the only material seen in the gas phase during this decomposition step.

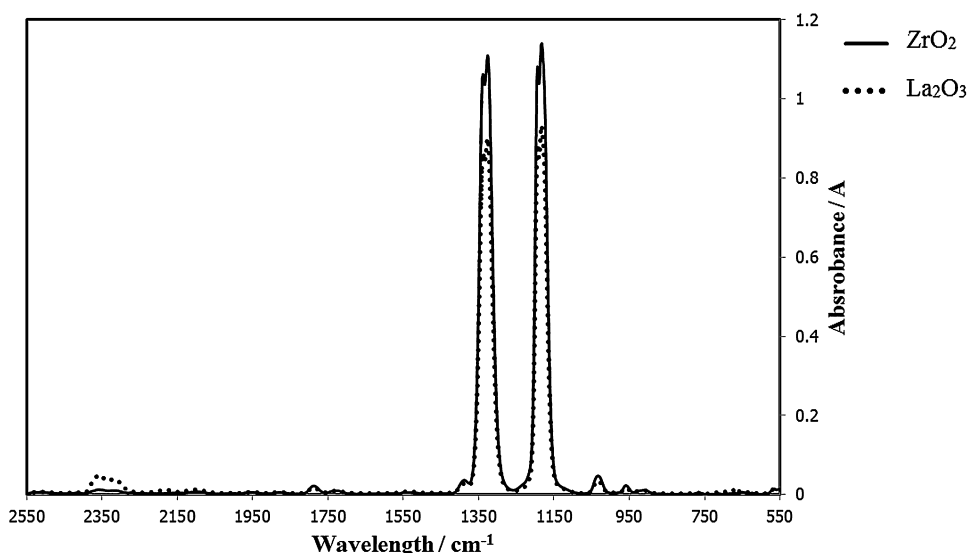


Fig. 10. Infrared spectra of the gas phase, taken at the point of maximum absorbance, for the decomposition of PTFE filled with ZrO_2 and La_2O_3 .

3. Conclusions

We have demonstrated that ZnO, NiO, Co₃O₄, Fe₂O₃, Mn₂O₃, Cr₂O₃, ZrO₂ and La₂O₃ are generally inert with respect to the degradation onset temperature and degradation rate of PTFE. We have also demonstrated that, except for ZrO₂, all these oxides undergo surface reactions with the PTFE pyrolysates to produce CO₂, with NiO and Cr₂O₃ also catalysing some small change in the gaseous composition, but producing predominantly TFE.

We have shown that CuO and V₂O₅ react in bulk with PTFE under pyrolysis conditions, greatly increasing the degradation rate and producing CO₂, with V₂O₅ decreasing the degradation onset temperature by 60 °C. CuO catalyses some change in the gas phase, forming short chain perfluoroalkanes. V₂O₅ produces an additional absorption band at 1028 cm⁻¹ which does not correspond to any of the known pyrolysis products.

Furthermore, we have demonstrated that Al₂O₃ shifts the gaseous product distribution to HFP and PFE and that the group 13 metal oxides decrease in reactivity with PTFE when going down the periodic table. A mechanism for the catalytic action of aluminium compounds with PTFE pyrolysates to form HFP is proposed.

4. Experimental

4.1. Sample preparation

ACS grade (purity > 99%) Al₂O₃, Ga₂O₃, In₂O₃, CuO, NiO and Fe₂O₃ were purchased from Sigma-Aldrich and used as received. Pharmaceutical grade ZnO (Ph. Eur., BP, USP, 99–100.5%) was purchased from Sigma Aldrich and used as received. High purity V₂O₅ (99.99% trace metal basis) was purchased from Sigma-Aldrich and used as received. Cr₂O₃ (purity ≥ 98%) and ZrO₂ (purity > 99%) was purchased from Merck and used as received. La₂O₃ (purity > 99%) was purchased from BDH Chemicals and used as received. PTFE 807NX originating from DuPont was used as received.

Mn₂O₃ was prepared by calcinating 10 g of MnO₂ in air at 800 °C for 24 h. The MnO₂ (ReagentPlus grade) was purchased from Sigma-Aldrich and used as received. The Co₃O₄ was prepared by calcinating 20 g of CoCO₃ in air at 800 °C for 24 h.

TGA samples were prepared by grinding 1 g of inorganic material with 1 g of PTFE in a mortar-and-pestle until the mixture appeared macroscopically homogeneous and stored in airtight glass vials.

4.2. Quantum chemical calculations

Quantum chemical calculations for the vanadium fluorides and -oxyfluorides were performed with the Spartan 06 software suite [15] using DFT (B3LYP) and the 6-31+G* basis set. The calculations were performed on a desktop computer supplied by Hewlett-Packard equipped with a 3.2 GHz Intel i7 2600 processor and 16 GB of memory.

4.3. TGA-FTIR analysis

TGA-FTIR experiments were conducted by placing approximately 50 mg of PTFE/filler mixture in α -alumina crucibles and pyrolysing it in a PerkinElmer TGA 4000 with the gaseous product transferred via a heated line to a PerkinElmer Spectrum 100 equipped with a heated transmission gas cell.

The pure PTFE samples were heated at a rate of 20 °C/min from 35 to 950 °C in an atmosphere of nitrogen flowing at 20 mL/min, while the filled samples were heated at a rate of 20 °C/min from 35 to 800 °C in an atmosphere of nitrogen flowing at 20 mL/min. The sampling port area immediately above the furnace was purged with nitrogen at a rate of 150 mL/min. The heated transfer line and IR gas cell were kept at 225 °C. Transfer of the sample from the TGA to the cell took place at a rate of 40 mL/min, thus diluting the sample with an extra 20 mL/min of nitrogen.

The spectrometer was set to take one scan every 6 s in the range of 4000–550 cm⁻¹ at a resolution of 4 cm⁻¹. The gas cell was fitted with KBr windows.

4.4. X-ray powder diffraction analysis

X-ray powder diffraction analysis was performed with a PANalytical X'Pert Powder X-ray diffractometer using Co radiation.

Acknowledgements

The authors would like to acknowledge the National Research Foundation of South Africa and the Department of Science and Technology's Fluorochemical Expansion Initiative for financially supporting this research.

References

- [1] G.J. Puts and P.L. Crouse, The influence of inorganic materials on the pyrolysis of polytetrafluoroethylene. Part 1: The sulfates and fluorides of Al, Zn, Cu, Ni, Co, Fe and Mn, 2014, 10.1016/j.jfluchem.2014.05.004.
- [2] Coblenz Society Inc., Evaluated infrared reference spectra, in: P.J. Linstrom, W.G. Mallard (Eds.), NIST Chemistry WebBook, NIST Standard Reference Database Number 69, National Institute of Standards and Technology, 2013.
- [3] R.C. Weast, Section B: Elements and inorganic compounds, in: CRC Handbook of Chemistry and Physics, CRC Press, Cleveland, OH, 1974.
- [4] Y. Maimaiti, M. Nolan, S.D. Elliott, Phys. Chem. Chem. Phys. 16 (2014) 3036–3046.
- [5] D.J. Ivy, M. Rigby, M. Baasandorj, J.B. Burkholder, R.G. Prinn, Atmos. Chem. Phys. 12 (2012) 7635–7645.
- [6] E.G. Hope, J. Chem. Soc. Dalton Trans. (1990) 723–725, <http://pubs.rsc.org/en/content/articlelanding/1990/dt/dt9900000723#!divAbstract>.
- [7] H. Selig, H.H. Claassen, J. Chem. Phys. 44 (1966) 1404–1406.
- [8] D.S. Su, R. Schlögl, Catal. Lett. 83 (2002) 115–119.
- [9] M. Digne, P. Sautet, P. Raybaud, P. Euzen, H. Toulhoat, J. Catal. 226 (2004) 54–68.
- [10] G.J. Puts, P.L. Crouse, B. Ameduri, Thermal degradation and pyrolysis of polytetrafluoroethylene, in: D.W. Smith, S.T. Iacono, S.S. Iver (Eds.), Handbook of Fluoropolymer Science and Technology, John Wiley & Sons, Inc., New York, 2014.
- [11] M.L. Pantoya, S.W. Dean, Thermochim. Acta 493 (2009) 109–110.
- [12] D.T. Osborne, M.L. Pantoya, Combust. Sci. Technol. 179 (2007) 1467–1480.
- [13] T. Onodera, K. Kawasaki, T. Nakakawaji, Y. Higuchi, N. Ozawa, K. Kurihara, M. Kubo, J. Phys. Chem. C 118 (2014) 5390–5396.
- [14] V.Y. Filatov, A.V. Murin, S.A. Kazienkov, S.V. Khitrin, S.L. Fuks, Russ. J. Appl. Chem. 84 (2011) 147–150.
- [15] Wavefunction Inc., Spartan 06, Wavefunction Inc., Irvine, CA, USA, 2006.